

Torsional chiral magnetic effect due to skyrmion textures in a Weyl superfluid $^3\text{He-A}$

Yusuke Ishihara, Takeshi Mizushima, Atsushi Tsuruta, and Satoshi Fujimoto
Department of Materials Engineering Science, Osaka University, Toyonaka 560-8531, Japan
 (Dated: January 28, 2019)

We investigate torsional chiral magnetic effect (TCME) induced by skyrmion-vortex textures in the A phase of the superfluid ^3He . In $^3\text{He-A}$, Bogoliubov quasiparticles around point nodes behave as Weyl fermions, and the nodal direction represented by the ℓ -vector may form a spatially modulated texture. ℓ -textures generate a chiral gauge field and a torsion field directly acting on the chirality of Weyl-Bogoliubov quasiparticles. It has been clarified by G. E. Volovik [Pi'sma Zh. Eksp. Teor. Fiz. **43**, 428 (1986)] that, if the ℓ -vector is twisted as $\hat{\ell} \cdot (\text{curl} \hat{\ell}) \neq 0$, the chiral gauge field is responsible for the chiral anomaly, leading to an anomalous current along ℓ . Here we show that, even if $\hat{\ell} \cdot (\text{curl} \hat{\ell}) = 0$, a torsion arising from ℓ -textures brings about contributions to the equilibrium currents of Weyl-Bogoliubov quasiparticles along $\text{curl} \ell$. This implies that while the anomalous current appears only for the twisted (Bloch-type) skyrmion of the ℓ -vector, the extra mass current due to TCME always exists regardless of the skyrmion type. Solving the Bogoliubov-de Gennes equation, we demonstrate that both Bloch-type and Néel-type skyrmions induce chiral fermion states with spectral asymmetry, and possess spatially inhomogeneous structures of Weyl bands in the real coordinate space. Furthermore, we discuss the contributions of Weyl-Bogoliubov quasiparticles and continuum states to the mass current density in the vicinity of the topological phase transition. In the weak coupling limit, continuum states give rise to backflow to the mass current generated by Weyl-Bogoliubov quasiparticles, which makes a non-negligible contribution to the orbital angular momentum. As the topological transition is approached, the mass current density is governed by the contribution of continuum states.

I. INTRODUCTION

Weyl semimetals have been attracting much attention because of the realization of chiral anomaly in condensed matter systems, which is experimentally detectable in various exotic transport phenomena such as the anomalous Hall effect, chiral magnetic effect, and negative magnetoresistance.¹⁻¹⁴ Chiral anomaly is the violation of conservation law of axial currents in the case with both electric and magnetic fields which are not orthogonal to each other. Its origin is attributed to monopole charge carried by Weyl points in the momentum space, which generate the Berry curvature, and are sources and drains of momentum generation. Recent experimental studies revealed the realization of chiral anomaly in Weyl semimetal materials via the observation of negative magnetoresistance.¹⁵⁻¹⁷

The notion of Weyl semimetals is naturally generalized to superconducting states.¹⁸ In superconductors with broken time-reversal symmetry such as chiral pairing states and non-unitary odd-parity pairing states, nodal excitations from point-nodes of the superconducting gap behave as Weyl fermions accompanying the Berry curvature. There are several candidate systems of Weyl superconductors and superfluids such as the A-phase of the superfluid ^3He ,¹⁹⁻²² URu₂Si₂,²³ the B-phase of UPt₃,²⁴ UCoGe,²⁵ and the B-phase of U_{1-x}Th_xBe₁₃.²⁶⁻²⁸ Since the Bogoliubov quasiparticles are the superposition of electrons and holes, the usual coupling with electromagnetic fields does not directly lead to chiral anomaly. However, it is still possible that in Weyl superconductors and Weyl superfluids, emergent electromagnetic fields arising from spatially inhomogeneous textures of the superconducting order parameter and its dynamics give rise to chiral anomaly phenomena. As a matter of fact, in 1997, more than ten years before the invention of the notion of Weyl semimetals, Bevan *et al.* observed momentum generation due to chiral anomaly in $^3\text{He-A}$ with skyrmion textures

of the ℓ -vector field,²⁹ which was motivated by pioneering theoretical works of Volovik and his collaborators.^{19,30-35} In the experiment,²⁹ the chiral anomaly was detected via the measurement of an extra force on skyrmion-vortices.

In this paper, we consider another chiral anomaly effect which is referred to as the torsional chiral magnetic effect (TCME). The TCME was originally proposed for magnetic Weyl semimetals with lattice dislocations.³⁶ Lattice dislocations give rise to torsion fields which cause emergent magnetic fields acting on Weyl fermions, and result in equilibrium currents flowing along the dislocation lines. The current induced by the torsion field is given by,

$$\mathbf{J}^{\text{TCME}} = \frac{ev_F \Lambda}{4\pi^2} \sum_{a=x,y,z} \mathbf{T}^a (p_{La} - p_{Ra}), \quad (1)$$

where v_F is the Fermi velocity, Λ is the momentum cutoff, $p_{L(R)a}$ ($a = x, y, z$) is the position of the Weyl point with left(right)-handed chirality in momentum space, and

$$(\mathbf{T}^a)^\mu = \frac{\epsilon^{\mu\nu\lambda}}{2} T_{\nu\lambda}^a, \quad (2)$$

where $T_{\nu\lambda}^a$ is torsion which can be realized in condensed matter systems by topological defects such as lattice dislocation and a skyrmion texture of magnetic order. In the case of superconductors, torsional magnetic fields arise from vortex textures of the superconducting order parameter or lattice strain, and hence, the negative thermal magnetoresistivity, that is, the anomalous enhancement of longitudinal thermal conductivity along the torsional magnetic field.³⁷

Here we focus on the A-phase of ^3He having a skyrmion-vortex as a promising platform for the TCME. The order parameter tensor, $A_{\mu i}$, that transforms as a vector with respect to index $\mu = x, y, z$ ($i = x, y, z$) under spin (orbital) rotations, is given by the complex form^{38,39}

$$A_{\mu i} = \Delta_A(T) \hat{d}_\mu (\hat{\mathbf{m}} + i \hat{\mathbf{n}})_i e^{i\varphi}, \quad (3)$$

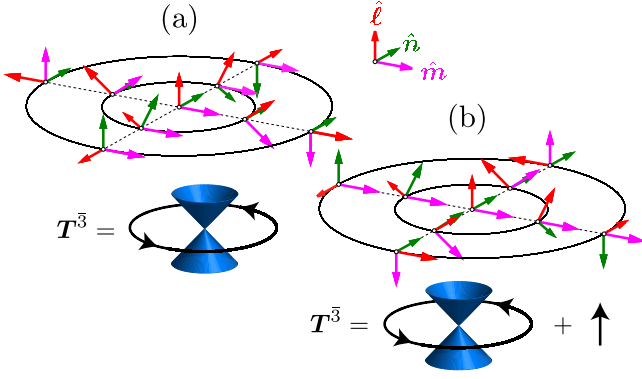


FIG. 1. Real-space skyrmion ℓ -textures and “torsional” magnetic fields acting on Weyl-Bogoliubov quasiparticles, $T^{\bar{3}} = \text{curl}\hat{\ell}$: (a) Néel-type skyrmion-vortex with $\alpha = 0$ and (b) Bloch-type skyrmion with $\alpha = \pi/2$ (see Eq. (27)). The former texture has $j^{\text{TCME}} \propto T^{\bar{3}}$ and $j^{\text{an}} = \mathbf{0}$, while the latter has nonvanishing $j^{\text{TCME}} \propto T^{\bar{3}}$ and $j^{\text{an}} \propto \hat{\ell}$.

where \hat{d} and (\hat{m}, \hat{n}) are unit vectors representing spin and orbital degrees of freedom in the superfluid vacuum, respectively. This is the Cooper-pair state with a definite orbital angular momentum represented by $\hat{\ell} \equiv \hat{m} \times \hat{n}$, and the ℓ -vector points to the nodal orientation at which Weyl-Bogoliubov quasiparticles reside. Owing to the spontaneously broken gauge-orbit symmetry, the rotation of the orbital part, $\hat{m} + i\hat{n}$, about $\hat{\ell}$ is equivalent to the U(1) phase rotation φ . This implies that the superfluid current can be generated by the texture of the triad $(\hat{m}, \hat{n}, \hat{\ell})$ without U(1) phase singularities. For rotating $^3\text{He-A}$, therefore, the ℓ -vector field spontaneously forms a skyrmion-like texture as a ground state,^{40–42} which is known as the Anderson-Toulouse vortex and the Mermion-Ho vortex (see Fig. 1).^{22,43–45} The ℓ -texture fields also appear in ^3He confined in a narrow cylinder.^{46,47} The relation between ℓ -textures and the mass current density at zero temperatures was derived by Mermin and Muzikar⁴⁸ as

$$\mathbf{j}^{\text{MM}} = \rho \mathbf{v}_s + \frac{\hbar}{4M} \text{curl} \rho \hat{\ell} - \frac{\hbar}{2M} C_0 \hat{\ell} (\hat{\ell} \cdot \text{curl} \hat{\ell}), \quad (4)$$

where ρ is the mass density of ^3He atoms, M is the mass, and $C_0 \approx \rho$ in the weak coupling approximation. The first term in Eq. (4) results from the superfluid velocity, and the second term arises from a variation of orbital angular momentum of the Cooper pair, $\hbar \hat{\ell}$, which resembles the electric current induced by a variation of the magnetization density in materials. The third term is the anomalous current referred to as j^{an} , which brings about a longstanding issue involved with the McClure-Takagi paradox.^{48–52} For twisted ℓ textures with $\hat{\ell} \cdot \text{curl} \hat{\ell} \neq 0$, j^{an} violates the McClure-Takagi relation that the ground state with an axially symmetric ℓ -texture has the total angular momentum per particle $L_z/N = \hbar/2$.

Using the semiclassical theory for Weyl-Bogoliubov quasiparticles, we here consider the contribution of the TCME to equilibrium mass flow in $^3\text{He-A}$ with skyrmion-vortices. The texture of the ℓ field brings both a chiral gauge field ($A^{\text{em}} \propto \hat{\ell}$) and torsion ($T^{\bar{3}}$) into Weyl-Bogoliubov quasiparticles. It has been discussed that, if $\hat{\ell}$ is twisted as $\hat{\ell} \cdot (\text{curl} \hat{\ell}) \neq 0$, the chiral

gauge field directly acting on the chirality of Weyl fermions leads to an anomalous current, $j^{\text{an}} \propto \hat{\ell} (\hat{\ell} \cdot \text{curl} \hat{\ell})$,^{19,30–35,53,54} which is the chiral-anomaly due to the emergent gauge field A^{em} . Here we show that a “torsion” field, $T^{\bar{3}} = \text{curl} \hat{\ell}$, arising from a texture of the triad $(\hat{m}, \hat{n}, \hat{\ell})$, gives rise to new torsional contributions as in Eq. (1). This is the torsional-anomaly aspect of the second term of Eq. (4). While j^{an} exists only for twisted (Bloch-type) skyrmions with $\hat{\ell} \cdot \text{curl} \hat{\ell} \neq 0$ (Fig. 1(b)), $j^{\text{TCME}} \propto \text{curl} \hat{\ell}$ is always finite regardless of the skyrmion type (Fig. 1(a)).

The Bogoliubov-de Gennes (BdG) equation enables a full quantum mechanical treatment of Bogoliubov quasiparticles and provides tractable and feasible approach to the vicinity of the topological phase transition. Solving the BdG equation, we demonstrate that Néel-type skyrmions induce chiral fermion states with spectral asymmetry, which are responsible for macroscopic mass flow along the azimuthal direction. The results are consistent with the semiclassical theory for Weyl-Bogoliubov quasiparticles with the torsional magnetic field, $T^{\bar{3}} = \text{curl} \hat{\ell}$. We also discuss the chiral fermion states and mass flow for both Néel-type and Bloch-type skyrmions in the light of the torsional magnetic field and discrete symmetries prevented by the skyrmion-vortex. Furthermore, we show that skyrmion ℓ -textures give rise to spatially inhomogeneous structures of the Weyl fermion band in addition to the torsional magnetic field⁵⁵; the position of Weyl points in the momentum space exhibits inhomogeneous textures in the real space. Lastly we discuss the contribution of the Weyl-Bogoliubov quasiparticles and continuum states to the mass current in the vicinity of the topological phase transition. In the weak coupling limit, continuum states give rise to backflow to the mass current generated by Weyl-Bogoliubov quasiparticles, which makes a non-negligible contribution to the orbital angular momentum. As the topological transition is approached, the mass current density is governed by the contribution of continuum states.

The organization of this paper is as follows. In Sec. II, we present semiclassical analysis for TCME in the case of Weyl superconductors/superfluids. In Sec. III, we describe the numerical method for solving the Bogoliubov-de-Gennes (BdG) equation for our purpose, and show the intrinsic features of Weyl-Bogoliubov quasiparticles in the presence of the ℓ -texture, such as spectral asymmetry and spatially inhomogeneous structures of the Weyl fermion band. In Sec. IV, we discuss the mass current density induced by the skyrmion texture from the viewpoint of the TCME. The final section is devoted to conclusion and discussion.

II. TORSIONAL CHIRAL MAGNETIC EFFECT AND SEMICLASSICAL ANALYSIS

A. Semiclassical equation of motion for Weyl-Bogoliubov quasiparticles

We consider the Bogoliubov-de Gennes (BdG) Hamiltonian for the Bogoliubov quasiparticles in the A-phase of the superfluid ^3He , i.e., a three-dimensional (3D) chiral $p + ip$ super-

fluid, with spatially varying gap structures such as skyrmion-like ℓ -vector textures of the Anderson-Toulouse vortex and the Mermin-Ho vortex. We apply the path integral formulation in a curved space with nonzero torsion which is induced by a vortex structure. In the Lagrangian in the Feynmann kernel, the spatially varying gap function is expressed as $A_{\mu i} p_i / p_F$ with the tensorial field $A_{\mu i}$ in Eq. (3). Here $\hat{\mathbf{m}}$ and $\hat{\mathbf{n}}$ are unit vectors for a local orthogonal frame which are perpendicular to the direction of the point nodes at $\mathbf{p} = s\mathbf{p}_0 \equiv s p_F \hat{\ell}$, where $s = \pm 1$ is the chirality of the Weyl points, and $\hat{\ell} = \hat{\mathbf{m}} \times \hat{\mathbf{n}}$ is the ℓ -vector. Δ is the superconducting gap, and p_F is the Fermi momentum. Then, the effective Lagrangian for Bogoliubov quasiparticles around $\mathbf{p} = s\mathbf{p}_0$ is given by

$$\mathcal{L}_s = \mathbf{p} \cdot \dot{\mathbf{r}} - \mathcal{H}_s(\mathbf{p}, \mathbf{r}), \quad (5)$$

with the Weyl-Bogoliubov Hamiltonian

$$\mathcal{H}_s(\mathbf{p}, \mathbf{r}) = s e_a^\mu V_b^a \tau^b (p_\mu - s p_{0\mu}), \quad (6)$$

where $V_b^a = \text{diag}[\frac{\Delta}{p_F}, \frac{\Delta}{p_F}, v]$ with v the Fermi velocity, τ^a is the Pauli matrix in the particle-hole space, and the vielbein e_a^μ is given by

$$(e_{\bar{1}}^\mu, e_{\bar{2}}^\mu, e_{\bar{3}}^\mu) = (m^\mu, n^\mu, \ell^\mu). \quad (7)$$

We use greek letter indices $\mu = 1, 2, 3$ as space indices for the laboratory frame, and roman letters $a = \bar{1}, \bar{2}, \bar{3}$ as indices for a local orthogonal frame. The Weyl Hamiltonian must obey the particle-hole symmetry

$$C \mathcal{H}_s(\mathbf{p}, \mathbf{r}) C^{-1} = -\mathcal{H}_{-s}(-\mathbf{p}, \mathbf{r}), \quad (8)$$

where $C = K\tau_1$ is the particle-hole conversion operator with τ_μ the Pauli matrices in the particle-hole space. The particle-hole symmetry guarantees that the Weyl point appears as a pair of \mathbf{p}_0 and $-\mathbf{p}_0$ and the pairwise Weyl points have opposite chirality, $s = \pm 1$.

For $^3\text{He-A}$ with $\mathbf{p}_0 = p_F \hat{\ell}$, the space-time modulation of the $\hat{\ell}$ -texture generates the emergent electromagnetic field, $\mathbf{B}^{\text{em}} = p_F \text{curl} \hat{\ell}$ and $\mathbf{E}^{\text{em}} = p_F \partial_t \hat{\ell}$, which directly act on the chirality of Weyl-Bogoliubov quasiparticles. Volovik and his collaborators^{19,30–35} found the chiral anomaly that the emergent field is responsible for the production of net quasiparticle momentum, $\partial_t \mathbf{P}_{\text{QP}} = \frac{1}{2\pi^2} \int d^3 r p_F \hat{\ell} \mathbf{E}^{\text{em}} \cdot \mathbf{B}^{\text{em}}$. As the quasiparticle momentum \mathbf{P}_{QP} is equivalent to the quasiparticle mass current in $^3\text{He-A}$, the violation of the quasiparticle momentum conservation is compensated by the extra mass current carried by the superfluid vacuum, that is, the anomalous current in Eq. (4), $\mathbf{j}^{\text{an}} = -\frac{\hbar}{2M} C_0 \hat{\ell} (\hat{\ell} \cdot \text{curl} \hat{\ell})$. Below, we show the another contribution of Weyl-Bogoliubov quasiparticles to Eq. (4) that the nontrivial torsion field due to the modulation of the vielbein, e_a^μ , is accompanied by the extra mass current along $\text{curl} \hat{\ell}$. This is the chiral magnetic effect due to the torsion field, which can be significant even if $\hat{\ell} \cdot \text{curl} \hat{\ell} = 0$.

Following the method developed in ref. 56, we obtain the effective Lagrangian for the upper band:

$$\mathcal{L}_s = p_\mu \dot{r}^\mu + \mathcal{E}_s + \mathcal{A}_{ps}^{+\mu} \dot{p}_\mu + \mathcal{A}_{rs\mu}^+ \dot{r}^\mu, \quad (9)$$

where the Berry connections are $\mathcal{A}_{ps}^{+\mu} = i \langle u_{s+} | \partial_{p_\mu} | u_{s+} \rangle$, and $\mathcal{A}_{rs\mu}^+ = i \langle u_{s+} | \partial_{r^\mu} | u_{s+} \rangle$ with $\mathcal{H}_s | u_{s+} \rangle = \mathcal{E}_s | u_{s+} \rangle$ and \mathcal{E}_s is the

single-particle energy of Weyl-Bogoliubov quasiparticles with chirality s .

The Berry connection and the Berry curvature in the momentum space characterizing Weyl fermions appear when one projects the state into the one of the two energy bands of $\mathcal{H}_s(\mathbf{p}, \mathbf{r})$. This approach is justified for Weyl semimetals, when the Fermi level crosses only one band, and the other band is well separated from the Fermi level. However, in the case of Weyl superconductors and Weyl superfluids, the Fermi level crosses the Weyl point at which the lower band touches the upper band, and thus, the projection procedure is not justified. Nevertheless, we exploit this approach to see qualitatively how the Berry curvature plays the role in the response against torsion fields.

In some cases with a spatially varying structure of the gap function such as a vortex, and the Mermin-Ho texture or the Anderson-Toulouse texture of the ℓ -vector, nonzero torsion appears. The torsion field is defined by

$$T_{\mu\nu}^a = \frac{\partial e_\nu^a}{\partial r^\mu} - \frac{\partial e_\mu^a}{\partial r^\nu}, \quad (10)$$

where e_a^μ is the inverse of e_a^μ .

In the case with nonzero torsion, the Euler-Lagrange equation for \mathbf{r} and $\dot{\mathbf{r}}$ is modified as,⁵⁷

$$\frac{d}{dt} \left(\frac{\partial \mathcal{L}}{\partial \dot{r}^\mu} \right) - \frac{\partial \mathcal{L}}{\partial r^\mu} = T_{\mu\lambda}^\nu \dot{r}^\lambda \frac{\partial \mathcal{L}}{\partial \dot{r}^\nu}, \quad (11)$$

with $T_{\mu\lambda}^\nu = e_\nu^\lambda T_{\mu\lambda}^a$, while that for \mathbf{p} and $\dot{\mathbf{p}}$ is not changed. Then, we obtain the equation of motion for the Weyl-Bogoliubov quasiparticles:

$$\frac{d\mathbf{r}}{dt} = \frac{\partial \mathcal{E}_s}{\partial \mathbf{p}} - \hat{\Omega}_{prs}^+ \cdot \frac{d\mathbf{r}}{dt} - \frac{d\mathbf{p}}{dt} \times \boldsymbol{\Omega}_{pps}^+ + \boldsymbol{\Omega}_{tps}^+, \quad (12)$$

$$\begin{aligned} \frac{d\mathbf{p}}{dt} = & -\frac{\partial \mathcal{E}_s}{\partial \mathbf{r}} + \hat{\Omega}_{rps}^+ \cdot \frac{d\mathbf{p}}{dt} + \frac{d\mathbf{r}}{dt} \times \boldsymbol{\Omega}_{rrs}^+ - \boldsymbol{\Omega}_{trs}^+ \\ & + \frac{d\mathbf{r}}{dt} \times \mathbf{T}^\mu (p_\mu + \mathcal{A}_{rs\mu}^+), \end{aligned} \quad (13)$$

where the Berry curvatures are,

$$\boldsymbol{\Omega}_{XXs}^+ = i \langle \nabla_X u_{s+} | \times | \nabla_X u_{s+} \rangle, \quad (14)$$

$$\boldsymbol{\Omega}_{tXs}^+ = i \langle (\partial_t u_{s+} | \nabla_X u_{s+}) - \langle \nabla_X u_{s+} | \partial_t u_{s+} \rangle \rangle, \quad (15)$$

$$(\hat{\Omega}_{prs}^+)_{\alpha\beta} = i \langle (\partial_{p_\alpha} u_{s+} | \partial_{r_\beta} u_{s+}) - \langle \partial_{r_\beta} u_{s+} | \partial_{p_\alpha} u_{s+} \rangle \rangle, \quad (16)$$

$$\hat{\Omega}_{rps}^+ = -(\hat{\Omega}_{prs}^+)^t, \quad (17)$$

with $\mathbf{X} = \mathbf{r}, \mathbf{p}$, and $(\mathbf{T}^\mu)^\nu = \frac{1}{2} \epsilon^{\nu\lambda\rho} T_{\lambda\rho}^\mu$. In Eqs. (12) and (13), all components of vectors are expressed in the laboratory frame. We can obtain similar equations also for the lower band. The Berry curvature is $\boldsymbol{\Omega}_{XYs}^- = -\boldsymbol{\Omega}_{XYs}^+$. It is noted that, as seen from (13), the torsion generates an effective magnetic field acting on quasiparticles. We denote it as

$$\mathcal{B} = \mathbf{T}^\mu (p_\mu + \mathcal{A}_{r\mu}^+) = \mathbf{T}^a (p_a + \mathcal{A}_{ra}^+). \quad (18)$$

In the following, we consider static inhomogeneity of the order parameter, and neglect Ω_{ips}^+ and Ω_{irs}^+ . Then, as follows from Eqs. (12) and (13),

$$\frac{d\mathbf{r}}{dt} = \frac{\partial \mathcal{E}_s}{\partial \mathbf{p}} + \frac{\partial \mathcal{E}_s}{\partial \mathbf{r}} \times \Omega_{pps}^+ - \left(\frac{\partial \mathcal{E}_s}{\partial \mathbf{p}} \cdot \Omega_{pps}^+ \right) \tilde{\mathcal{B}} - \hat{\Omega}_{prs}^+ \cdot \frac{d\mathbf{r}}{dt} + (\Omega_{pps}^+ \cdot \tilde{\mathcal{B}}) \frac{d\mathbf{r}}{dt}, \quad (19)$$

$$\frac{d\mathbf{p}}{dt} = -\frac{\partial \mathcal{E}_s}{\partial \mathbf{r}} + \frac{d\mathbf{r}}{dt} \times \tilde{\mathcal{B}} + \left(\frac{\partial \mathcal{E}_s}{\partial \mathbf{r}} \cdot \tilde{\mathcal{B}} \right) \Omega_{pps}^+ + \hat{\Omega}_{rps}^+ \cdot \frac{d\mathbf{p}}{dt} + (\Omega_{pps}^+ \cdot \tilde{\mathcal{B}}) \frac{d\mathbf{p}}{dt}, \quad (20)$$

where $\mathbf{v}_{ps} = \partial \mathcal{E}_s / \partial \mathbf{p}$, and $\tilde{\mathcal{B}} = \Omega_{rr}^+ + \mathcal{B}$. In Eq. (19), the third term of the right-hand side represents the chiral magnetic effect, and the contribution proportional to \mathcal{B} corresponds to the torsional chiral magnetic effect found in ref. 36. The third term of the right-hand side of Eq. (20) is associated with chiral anomaly; i.e. the momentum is generated or annihilated at the Weyl points when both an effective magnetic field and a bias potential are applied in the same direction. It has recently been found that from Eqs. (19) and (20) the torsional chiral magnetic effect arising from a U(1) phase vortex or lattice strain leads to the negative thermal magnetoresistivity, that is, the anomalous enhancement of longitudinal thermal conductivity along the vortex line.³⁷

B. Torsional chiral magnetic effect due to ℓ -textures

The current density induced by the torsional field is written as⁵⁶

$$\mathbf{j}_\mu^{\text{TCME}} = \sum_{s,\pm} \int \frac{d^3k}{(2\pi)^3} (\mathbf{v}_{ks}^\pm \cdot \Omega_{kks}^\pm) f(\mathcal{E}_s) \mathcal{B}^\mu, \quad (21)$$

where $f(\epsilon) = 1/(e^{\epsilon/T} + 1)$ is the Fermi distribution function. Equation (21) reproduces the current expression based on the linear response of the effective action for Weyl-Bogoliubov quasiparticles with respect to the torsional magnetic field.³⁶ The effective Hamiltonian in Eq. (6) possesses anisotropic dispersion of Weyl-Bogoliubov quasiparticles and the Berry curvature is

$$\Omega_{kks}^\pm = \pm s \left(\frac{1}{p_F \xi} \right)^2 \frac{\mathbf{k} - s\mathbf{k}_0}{2|\tilde{\mathbf{k}} - s\tilde{\mathbf{k}}_0|^3}, \quad (22)$$

where we have introduced $\tilde{k}_b = v_b^a k_a / v_F$ and $\xi = v_F / \Delta_A$. We also introduce a momentum cutoff $|\tilde{\mathbf{k}} - s\tilde{\mathbf{k}}_0| < b\Delta_A / v_F \equiv \Lambda$ for Weyl-Bogoliubov quasiparticles with the chirality s , where $b \sim 1$. A nonzero torsional magnetic field leads to the equilibrium current

$$\mathbf{j}^{\text{TCME}} = \frac{v_F p_F \Lambda}{2\pi^2} \mathbf{T}^{\bar{3}}, \quad (23)$$

where we utilize the particle-hole symmetry in Eq. (8).

As seen from Eqs. (10) and (18), in the A-phase of ^3He , a torsional magnetic field is generated by the rotation of the Weyl points, $\mathbf{p}_0 = p_F \hat{\ell}$, as

$$\mathbf{T}^{\bar{3}} = \text{curl} \hat{\ell}. \quad (24)$$

The real space texture of the ℓ vector field is thermodynamically stable in superfluid ^3He -A under rotation. This is a consequence of the broken gauge-orbit symmetry in the superfluid vacuum; the U(1) phase rotation in Eq. (3) is equivalent to the rotation of the orbital part $\hat{\mathbf{m}} + i\hat{\mathbf{n}}$ about $\hat{\ell}$. Therefore, the supercurrent can be generated by a variation of $(\hat{\mathbf{m}}, \hat{\mathbf{n}}, \hat{\ell})$ without a U(1) phase singularity. The ℓ -texture spontaneously emerges in ^3He -A under rotation, and continuous skyrmion-like textures provide an elementary building-block for a variety of coreless vortices with the spatially uniform superfluid density.^{40,41} Here we consider skyrmion-vortices with the Néel-type and Bloch-type ℓ textures as in Fig. 1.

Let us now clarify the torsional field induced by skyrmion vortices. It is convenient to express the orbital part of the order parameter tensor in Eq. (3) in terms of Euler angles α, β, γ as $\hat{\mathbf{m}} + i\hat{\mathbf{n}} = e^{-i\gamma}(\hat{\mathbf{m}}' + i\hat{\mathbf{n}}')$, where

$$\hat{\mathbf{m}}' = \cos \beta \cos \alpha \hat{x} + \cos \beta \sin \alpha \hat{y} - \sin \beta \hat{z}, \quad (25)$$

$$\hat{\mathbf{n}}' = -\sin \alpha \hat{x} + \cos \alpha \hat{y}, \quad (26)$$

and $\hat{\ell} = \cos \alpha \sin \beta \hat{x} + \sin \alpha \sin \beta \hat{y} + \cos \beta \hat{z}$. The texture is assumed to be translationally invariant along the z axis and be axially symmetric. The axisymmetric skyrmion texture requires the Euler angles to obey $\alpha \equiv \theta + \alpha_0(r)$, $\gamma = -n\theta$ ($n \in \mathbb{Z}$), and $\beta \equiv \beta(r)$, where r is the distance from the center of the vortex and θ is the azimuthal angle. For the real-space ℓ -vector field with axial symmetry, therefore, the parametrization reduces to

$$\hat{\ell} = \sin \beta \cos \alpha_0 \hat{r} + \sin \beta \sin \alpha_0 \hat{\theta} + \cos \beta \hat{z}, \quad (27)$$

where $\hat{\ell} \equiv \hat{\ell}(r)$, $\beta \equiv \beta(r)$, and $\alpha_0 \equiv \alpha_0(r)$. The bending angle is a monotonic function on r which obeys $\beta(r) = 0$ at $r = 0$ and $\beta(r) = \pi/2$ at $r = R$, where R determines the size of the skyrmion texture. In Fig. 1, we present the texture of $(\hat{\mathbf{m}}, \hat{\mathbf{n}}, \hat{\ell})$ in the skyrmion-vortex with $n = 1$: (a) the Néel-type skyrmion with $\alpha = 0$ and (b) the Bloch-type skyrmion with $\alpha = \pi/2$. From Eqs. (27) and (7), the nonzero torsion field in Eq. (10) can be generated by a skyrmion ℓ texture of continuous vortices as

$$\mathbf{T}^{\bar{3}} = \beta' \sin \beta \hat{\theta} + \left[\left(\beta' \cos \beta + \frac{1}{r} \sin \beta \right) \sin \alpha + \frac{\alpha'}{r} \sin \beta \cos \alpha \right] \hat{z}, \quad (28)$$

where $\alpha' \equiv \partial \alpha / \partial r$ and $\beta' \equiv \partial \beta / \partial r$. As shown in Fig. 1, the Néel-type skyrmion texture for $\alpha = 0$ generates the toroidal torsional magnetic field in the xy plane, while the Bloch-type skyrmion for $\alpha \neq 0$ is accompanied by the nonzero torsion field along the z axis.

Using the particle density, $\rho = p_F^3 / 3\pi^2$, the TCME is recast into

$$\mathbf{j}^{\text{TCME}} = \left(\frac{b'}{p_F \xi} \right) \frac{\hbar}{4M} \rho \text{curl} \hat{\ell}, \quad (29)$$

where $b' \sim 1$ is the dimensionless quantity associated with the cutoff of the Weyl cone. The skyrmion texture with Eq. (27) therefore gives rise to the in-plane circulating current and the out-of-plane current, depending on α . We note that \mathbf{j}^{TCME} in Eq. (29) corresponds to the Weyl-Bogoliubov quasiparticle contributions to the second term of the right-hand side of the equilibrium current density in Eq. (4). This is distinct from the chiral anomaly effect due to the emergent electromagnetic fields considered in previous studies.^{19,30} In Sec. IV, we will discuss the temperature dependence of the equilibrium current density based on the full quantum mechanical calculation.

III. CHIRAL FERMIONS IN SKYRMION-VORTEX

In this section, we show the emergence of chiral fermions in superfluid $^3\text{He-A}$ with skyrmion ℓ -textures. Beyond the semi-classical effective theory, we here utilize the BdG equation which is the fully quantum-mechanical equation for Bogoliubov quasiparticles in superfluid $^3\text{He-A}$.

We start with the Hamiltonian for the equal spin pairing state, $A_{\mu i}(\mathbf{r}) = \Delta_i(\mathbf{r})\hat{d}_\mu$,

$$\mathcal{H} = \int d\mathbf{r} \psi^\dagger(\mathbf{r}) \varepsilon(-i\nabla) \psi(\mathbf{r}) + \frac{1}{2} \int d\mathbf{r} \left[\psi^\dagger(\mathbf{r}) \left\{ \Delta_j(\mathbf{r}), \frac{i}{p_F} \partial_j \right\} \psi^\dagger(\mathbf{r}) + \text{h.c.} \right], \quad (30)$$

where ψ_a and ψ_a^\dagger denote the fermionic field operators. As $^3\text{He-A}$ is the equal spin pairing state, we omit the spin degrees of freedom. The single-particle Hamiltonian density represents fermions with mass M , $\varepsilon(-i\nabla) = -\nabla^2/2M - \mu$. The repeated Roman and Greek indices imply the sum over the spin degrees of freedom and (x, y, z) , respectively.

Now, let us introduce the Bogoliubov transformation of the fermion operator $\Psi \equiv [\psi, \psi^\dagger]^T$,

$$\Psi(\mathbf{r}) = \sum_{E>0} \left[\varphi_E(\mathbf{r}) \eta_E + C \varphi_E(\mathbf{r}) \eta_E^\dagger \right], \quad (31)$$

where η_E and η_E^\dagger stand for Bogoliubov quasiparticle operators with the energy E that satisfy fermionic anticommutation relations. We notice that Eq. (31) obeys the particle-hole symmetry, $C\Psi = \Psi$, with $C = \tau_x K$ where K is the complex conjugation operator. Substituting Eq. (31) into the Hamiltonian (30), one obtains the Bogoliubov-de Gennes (BdG) equations

$$\mathcal{H}_{\text{BdG}}(\mathbf{r}) \varphi_E(\mathbf{r}) = E \varphi_E(\mathbf{r}), \quad (32)$$

with

$$\mathcal{H}_{\text{BdG}}(\mathbf{r}) = \begin{pmatrix} \varepsilon(-i\nabla) & \frac{1}{2} \sum_j \left\{ \Delta_j, \frac{i}{p_F} \partial_j \right\} \\ \frac{1}{2} \sum_j \left\{ \Delta_j^*, \frac{i}{p_F} \partial_j \right\} & -\varepsilon(-i\nabla) \end{pmatrix}, \quad (33)$$

where $\{, \}$ denotes an anti-commutator. To make the Bogoliubov transformation canonical, the quasiparticle wavefunction must satisfy the orthonormal conditions $\int d\mathbf{r} \varphi_E^\dagger(\mathbf{r}) \varphi_{E'}(\mathbf{r}) = \delta_{E,E'}$.

A. Symmetry of Weyl-Bogoliubov quasiparticles in skyrmion-vortices

To clarify the symmetry of Bogoliubov quasiparticles in the presence of a skyrmion ℓ -texture, we start with the symmetry group relevant to the classification of axisymmetric vortices in superfluid ^3He ,

$$G_v = D_{\infty,h} \times t^z \times T \times U(1)_\varphi, \quad (34)$$

where $D_{\infty,h}$ contains the group of rotations about the vortex line (\hat{z}), rotations about an axis perpendicular to \hat{z} , and space inversion, and t^z represents the translational symmetry of the skyrmion-vortex along \hat{z} . The time reversal symmetry, T , transforms the order parameter tensor as $A_{\mu i} \mapsto A_{\mu i}^*$. The generator of the continuous rotation symmetry about \hat{z} is expressed as $e^{i\hat{Q}\varphi}$, where $\hat{Q} \equiv \hat{L}_z - n\hat{I}$ ($n \in \mathbb{Z}$) is the combination of the orbital angular momentum operator \hat{L}_z and the $U(1)$ phase rotation operator. The order parameter for axisymmetric vortices satisfies $\hat{Q}\Delta_j(\mathbf{r}) = 0$. For the skyrmion-vortex states in Fig. 1, the orbital components of the order parameter are given by

$$\Delta(\mathbf{r}) = \Delta_A(T) e^{i\theta} [\hat{m}'(r) + i\hat{n}'(r)], \quad (35)$$

with Eqs. (25) and (26). In this paper, we focus on the $n = 1$ case.

It is convenient to transform Eq. (35) into the eigenstates of the orbital angular momentum $l = +1, 0, -1$ as $(\Delta_{+1}, \Delta_0, \Delta_{-1})$. This transforms the off-diagonal component of Eq. (33) as $\sum_j \{ \Delta_j, \frac{i}{p_F} \partial_j \} \mapsto \sum_l \{ \Delta_l(\mathbf{r}), \mathcal{Y}_{1,l}(\boldsymbol{\theta}) \}$, where $\mathcal{Y}_{L,l}(\boldsymbol{\theta})$ is the spherical harmonic function of degree L obtained by replacing $\hat{\mathbf{p}} \rightarrow -i\boldsymbol{\partial}/p_F$. The phase factor $e^{i\theta}$, which appears in $\mathcal{Y}_{1,l}$, is compensated by the winding of (\hat{m}', \hat{n}') in $\Delta_l(\mathbf{r})$ and the $U(1)$ phase factor $e^{i\theta}$ is factorized from the off-diagonal component in Eq. (33) at all. The quasiparticle wavefunctions are then factorized in terms of the azimuthal quantum number $m \in \mathbb{Z}$ and axial quantum number k as

$$\varphi_E(\mathbf{r}) = e^{ikz} \begin{pmatrix} u_{nmk}(r) e^{im\theta} \\ v_{nmk}(r) e^{i(m-1)\theta} \end{pmatrix}. \quad (36)$$

Here we impose the periodic boundary condition along the axial direction, $\varphi_E(x, y, z) = \varphi_E(x, y, z + Z)$, which implies $k = 2\pi n_z/Z$ with $n_z \in \mathbb{Z}$. By using the factorization in Eq. (36), Eq. (33) is reduced to the one-dimensional differential equation for $[u_{nmk}(r), v_{nmk}(r)]$, where the set of the quantum numbers is given as (n, m, k) . The differential equation in the cylindrical coordinate is solved by expanding the wavefunctions with the orthonormal basis. The set of the basis functions is constructed with the Bessel function and the i -th zeros of the ν Bessel function, $J_\nu(r)$ and α_ν^i , as $\{C_j^\nu J_\nu(\alpha_j^\nu r/R)\}_{j=1, \dots, N}$, where C_j^ν and N denote the normalization constant and the number of the orthonormal functions, respectively. This imposes the rigid wall boundary condition, $u_{nmk}(r=R) = v_{nmk}(r=R) = 0$. The Bessel function expansion then reduces Eq. (33) to the $2N \times 2N$ eigenvalue equation.⁵⁸⁻⁶⁰ We take $R = 50-200k_F^{-1}$ and $N = 600$.

Apart from the continuous symmetry, there are discrete symmetries, which leave axisymmetric vortex order parameter invariant. First we note that the BdG Hamiltonian in

TABLE I. Classification of skyrmion-vortex textures in terms of the discrete symmetries. The ‘‘Néel’’, ‘‘Bloch’’, and ‘‘twist’’ textures correspond to $\alpha = 0$, $\alpha = \pi/2$, and $\alpha(r)$, respectively, \mathcal{M} is the torsional magnetic field due to the ℓ -texture, and ‘‘ZES’’ denotes the distribution of the zero energy states.

class	ℓ -texture	P_1	P_2	P_3	$\mathcal{B} \parallel \hat{z}$	ZES
v	Néel	–	$\sqrt{\quad}$	–	–	flat
w	Bloch	–	–	$\sqrt{\quad}$	$\sqrt{\quad}$	point
uvw	twist	–	–	–	$\sqrt{\quad}$	point

Eq. (33) always satisfies the particle-hole symmetry

$$C\mathcal{H}_{\text{BdG}}(\mathbf{r})C^{-1} = -\mathcal{H}_{\text{BdG}}(\mathbf{r}). \quad (37)$$

This results in relation (8). The symmetry guarantees that the eigenstate of the BdG equation must appear as a pair of the positive and negative energy states. The positive energy state with $E_n(m, k)$ and $\varphi_{n,m,k}(r) \equiv [u_{nmk}(r), v_{nmk}(r)]^T$ has the particle-hole symmetric partner with $-E_n(-m+1, -k)$ and $C\varphi_{n,-m+1,-k}(r)$.

The other discrete symmetries relevant to the vortex classification are given by three operators, $\{P_1, P_2, P_3\}$.^{22,40,61,62} P_1 is the space inversion operator. The order-2 antiunitary operator, P_3 , is the combination of the time reversal symmetry and π -rotation about any axis perpendicular to the vortex line. The P_2 symmetry is defined as $P_2 = P_1P_3$, which is the combination of the time-reversal symmetry and mirror reflection symmetry in a plane that contains the vortex line. Axisymmetric continuous vortices with skyrmion-like ℓ -texture are classified in terms of these discrete symmetries into three categories: v -, w -, and uvw -vortices.⁴⁰ The order parameters of the v - and w -vortices are invariant under the P_2 and P_3 symmetry, respectively, while the uvw -vortex class spontaneously breaks all the discrete symmetries.

Let us define the operator $M = i\sigma_y$ that denotes the mirror reflection in the xz plane. The operator flips the spin, momentum, and spatial coordinate as $\sigma \mapsto (-\sigma_x, \sigma_y, -\sigma_z)$, $\mathbf{k} \mapsto (k_x, -k_y, k_z)$, and $\mathbf{r} \mapsto (x, -y, z)$, respectively. The P_2 operator is defined as the combination of M and the time-reversal operator $\mathcal{T} = -i\sigma_y K$. For $\hat{\mathbf{d}} \parallel \hat{z}$, the P_2 operator flips the triad as $\hat{\mathbf{m}}(r, \theta, z) \mapsto [\hat{m}_x(r, -\theta, z), -\hat{m}_y(r, -\theta, z), \hat{m}_z(r, -\theta, z)]$, $\hat{\mathbf{n}}(r, \theta, z) \mapsto [-\hat{n}_x(r, -\theta, z), \hat{n}_y(r, -\theta, z), -\hat{n}_z(r, -\theta, z)]$, and $\hat{\ell}(r, \theta, z) \mapsto [\hat{\ell}_x(r, -\theta, z), -\hat{\ell}_y(r, -\theta, z), \hat{\ell}_z(r, -\theta, z)]$. Similarly, the P_3 symmetry relates the triad at (r, θ, z) to $(\hat{m}_x, -\hat{m}_y, \hat{m}_z)$, $(-\hat{n}_x, \hat{n}_y, -\hat{n}_z)$, and $(\hat{\ell}_x, -\hat{\ell}_y, \hat{\ell}_z)$ at $(r, \pi - \theta, -z)$. The Néel-type skyrmion-vortex (v -vortex) with $\alpha = 0$ in Fig. 1(a) spontaneously breaks the P_1 symmetry but maintains the P_2 symmetry. The vortex state with the Bloch-type skyrmion texture ($\alpha = \pi/2$) in Fig. 1(b) belongs to the w -vortex class with P_3 symmetry. The uvw -vortex class can be realized by twisting the skyrmion ℓ -texture so as to satisfy the conditions $\alpha(0) = \pi/2$ and $\alpha(R) = 0$. In Table I, we summarize the possible classification of skyrmion-vortices in terms of the discrete symmetries.

The P_2 symmetry imposes an important constraint on the energy spectrum of the Bogoliubov quasiparticles so as to prohibit the equilibrium current along the axial direction. Ax-

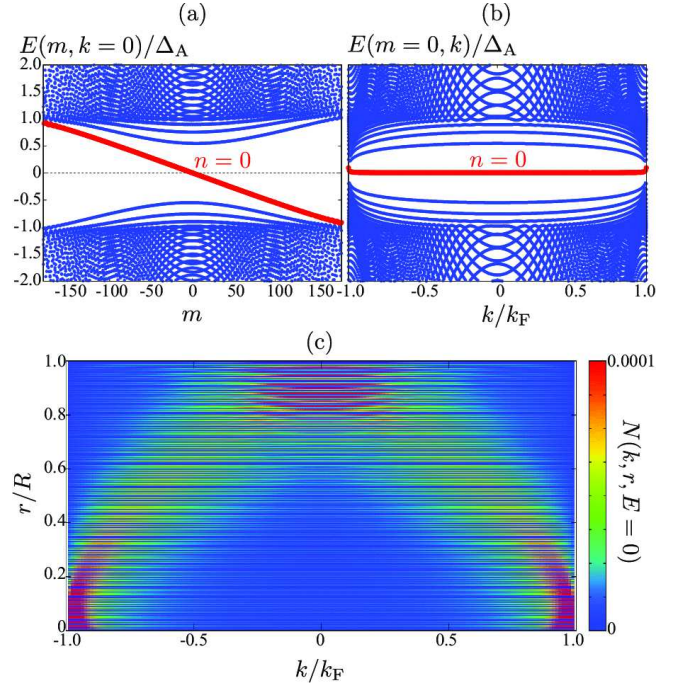


FIG. 2. Bogoliubov quasiparticle spectra for Néel-type skyrmion ($\alpha = 0$) at $E_n(m, k = 0)$ (a) and $E_n(m = 0, k)$ (b). (c) k -resolved zero-energy local density of states, $N(k, r, E = 0)$ representing the spatial distribution of the chiral fermion. We fix $R = 200k_F^{-1}$ and $p_F\xi = 20$.

isymmetric v -vortices must satisfy the relation

$$E_n(m, k) = E_n(m, -k) = -E_n(-m+1, -k). \quad (38)$$

The first equality results from the P_2 symmetry, while the second equality reflects the particle hole symmetry. Hence, the Bogoliubov quasiparticle spectrum in the Néel-type skyrmion-vortex with $\alpha = 0$ is an even function on k and the current flow along \hat{z} is prohibited. In contrast, as the P_3 symmetry does not impose any constraints on the eigenvalues, the Bloch-type and twisted skyrmion ℓ -textures may generate the equilibrium current along the axial direction.

B. Chiral fermions and real space texture of Weyl points

Let us consider the superfluid $^3\text{He-A}$ confined in a cylinder with radius R . The triad $(\hat{\mathbf{m}}, \hat{\mathbf{n}}, \hat{\ell})$ parameterized as Eqs. (25), (26), and (27) slowly varies from $\hat{\ell} = \hat{z}$ at $r = 0$ to $\hat{\ell} = \hat{r}$ at $r = R$. Hence, the bending angle is given by $\beta(r) = \frac{\pi}{2R}r$. We here set the angle as $\alpha(r) = 0$ for the Néel-type skyrmion (v -vortex) and $\alpha(r) = \frac{\pi}{2}(1 - r/R)$ for the twisted skyrmion (uvw -vortex). The size of the half-skyrmion is set to be larger than the superfluid coherence length ξ , $R \gtrsim 10\xi$ where $\xi \equiv v_F/\Delta_A > k_F^{-1}$.

In Fig. 2, we show the Bogoliubov quasiparticle spectra obtained by diagonalizing Eq. (33) with the Néel-type skyrmion textures (v -vortex). The Bogoliubov spectrum is asymmetric with respect to the azimuthal quantum number m and lowest branch ($n = 0$) crosses the zero energy. As mentioned

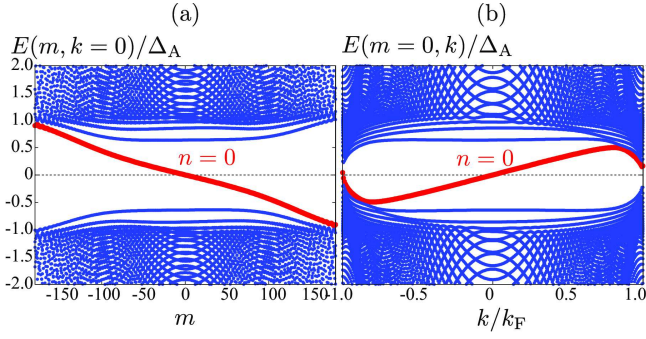


FIG. 3. Bogoliubov quasiparticle spectra for twisted skyrmion ($\alpha = \pi/2(1 - r/R)$) at $E_n(m, k = 0)$ (a) and $E_n(m = 0, k)$ (b). We fix $R = 200k_F^{-1}$ and $p_F\xi = 20$.

in Sec. II, the Weyl-Bogoliubov quasiparticles around point nodes experience the torsional magnetic field $\mathbf{T}^3 = \nabla \times \boldsymbol{\ell}$. For the Néel-type ℓ skyrmion with $\alpha = 0$, the toroidal torsional magnetic field, $\mathbf{T}^3 \propto \hat{\theta}$, leads to the emergence of the Landau levels linearly dispersing from $m = 0$. The lowest energy branch crossing the Fermi level in Fig. 2(a) is asymmetric with respect to m

$$E_0(m, k) = -v \left(m - \frac{1}{2} \right), \quad (39)$$

which is identified as the chiral fermion due to the emergent toroidal field. The group velocity, $-v < 0$, is an order of Δ_A/k_F . Figure 2(b) shows the dispersion of the Bogoliubov spectrum with respect to the axial momentum k at $m = 0$, which satisfies the P_2 symmetry constraint in Eq. (38). The almost flat dispersion of the lowest eigenstates indicates that the chiral branch in Eq. (39) exists within $|k| < k_F$. Hence, the spectral asymmetry in the Néel-type skyrmion-vortex leads to the equilibrium current along the azimuthal direction and the P_2 symmetry prohibits the flow along the axial direction.

To capture the spatial distribution of the chiral fermions, we show in Fig. 2(c) the k_z -resolved zero-energy local density of states, $N(k_z, r, E)$,⁶³

$$N(k, r, E) = \sum_{E>0}' \left[|u_{nmk}(r)|^2 \delta(E - E_n(m, k)) + |v_{nmk}(r)|^2 \delta(E + E_n(m, k)) \right], \quad (40)$$

where $\sum_{E>0}'$ stands for the sum over (n, m) that satisfies $E_n(m, k) > 0$. The peak amplitude in the plane (k, r) shifts from $r = R$ at $k = 0$ to $r = 0$ at $k = \pm k_F$. The spectral evolution reflects the spatial profiles of the Néel-type skyrmion ℓ -texture that smoothly tilts from the axial direction to the Néel-type direction. Therefore, the asymmetric branch crossing $E = 0$ in Fig. 2 is attributed to the Weyl-Bogoliubov quasiparticles bound to the Weyl points and the ℓ -vector texture leads to spatially inhomogeneous structures of Weyl bands in the real coordinate space.

Figure 3 shows the Bogoliubov quasiparticle spectra for the twisted skyrmion ℓ -texture. It is seen that the chiral fermion branch with the spectral asymmetry exists in the k direction

as well as the azimuthal momentum m . In order to satisfy the rigid wall boundary condition, $\hat{\boldsymbol{\ell}} = \hat{\mathbf{r}}$, at $r = R$, we set the azimuthal angle as $\alpha(r) = (1 - r/R)\pi/2$. The resulting ℓ texture generates the torsional magnetic field long the axial direction in addition to the azimuthal direction. This is categorized to the uvw -vortex class which holds neither the P_2 symmetry nor P_3 symmetry. The symmetry relation in Eq. (38) can be violated and the spectral asymmetry along k is responsible for the equilibrium current along the axial direction.

IV. TORSIONAL CHIRAL MAGNETIC EFFECT AND MASS CURRENT IN SKYRMION-VORTEX

In the previous section, we have demonstrated that the chiral fermion branches emerge in the Bogoliubov quasiparticle spectrum under skyrmion-like ℓ -textures. Using the full quantum mechanical BdG equation, in this section, we show that low-lying Weyl-Bogoliubov quasiparticles dominantly contribute to the current density in the weak coupling regime, while the contributions from continuum states become significant as the topological phase transition is approached. Here we introduce the dimensionless parameter $p_F\xi = 2E_F/\Delta_A$ so as to quantify the quantum corrections to the quasiclassical limit ($p_F\xi \gg 1$).

A. Néel-type skyrmion

We define the mass current density $\mathbf{j}(\mathbf{r})$ as the linear response of the thermodynamic potential with respect to an infinitesimal flow \mathbf{v} , $j_\mu = (\delta\langle \mathcal{H} \rangle / \delta v_\mu)_{v=0}$, where the Hamiltonian under a homogeneous velocity field is given by a Galilean transformation $-i\nabla \mapsto -i\nabla - M\mathbf{v}$. The current density is then given by $j_\mu(\mathbf{r}) = -i\langle \psi^\dagger(\mathbf{r})\partial_\mu\psi(\mathbf{r}) - \psi(\mathbf{r})\partial_\mu\psi^\dagger(\mathbf{r}) \rangle$. In terms of the Bogoliubov quasiparticle wavefunctions $\boldsymbol{\varphi}_E = [u_E, v_E]^T$, this is rewritten to

$$j_\mu(\mathbf{r}) = 2 \sum_{E>0} \left[\text{Im} \left\{ u_E^*(\mathbf{r}) \partial_\mu u_E(\mathbf{r}) \right\} f(E) + \text{Im} \left\{ v_E(\mathbf{r}) \partial_\mu v_E^*(\mathbf{r}) \right\} f(-E) \right], \quad (41)$$

where the factor “2” arises from the spin degeneracy in the equal spin pairing state and $f(E) = 1/(e^{E/T} + 1)$ is the Fermi distribution function at temperature T . Owing to the particle-hole symmetry, the azimuthal current density in Eq. (41), or the angular momentum density $(\mathbf{r} \times \mathbf{j})_z = r j_\theta(r)$, is recast into

$$r j_\theta(r) = -2 \sum_{E>0} (m-1) |v_E(r)|^2 = 2 \sum_{E<0} m |u_E(r)|^2, \quad (42)$$

at $T = 0$, where $n(\mathbf{r}) = 2\langle \psi^\dagger \psi \rangle$ is the particle density and $\sum_{E>0}$ stands for the sum over (n, m, k) within $E_n(m, k) > 0$. As shown in Fig. 2(a), the chiral fermion states with $m \geq 1$ have negative energy and thus are occupied at $T = 0$. These chiral fermion states make a positive contribution to the mass current density along the azimuthal direction, $j_\theta(r)$. In the Néel-type skyrmion-vortex, therefore, they produce an azimuthal mass current in the same sense as the torsional field, $\mathbf{T}^3 = \text{curl} \hat{\boldsymbol{\ell}}$.

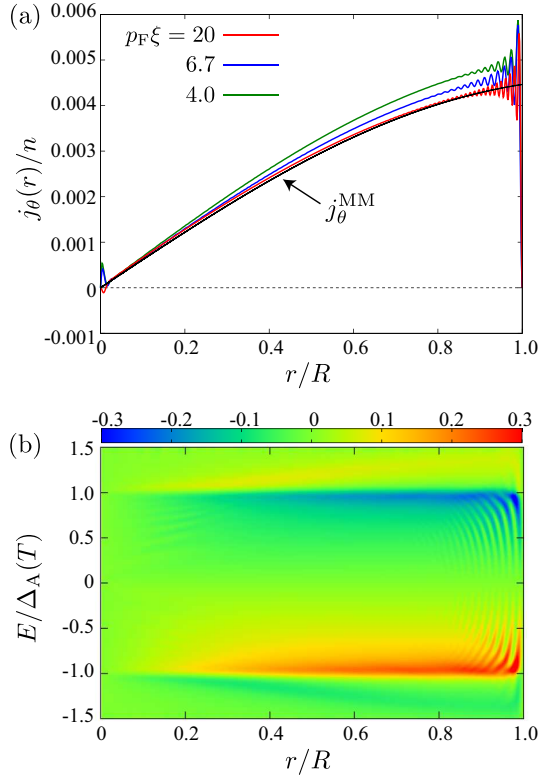


FIG. 4. (a) Current density in the Néel-type skyrmion-vortex, where n is the particle density. (b) E -resolved current density profile, $j_\theta(r, E)$, for $k_F\xi = 20$. Here we fix $T = 0$, $R = 200k_F^{-1}$, and $\mu = E_F$.

In Fig. 4(a), we plot the current density, $j_\theta(r)$, in the Néel-type skyrmion-vortex (v -vortex) at $T = 0$ for $p_F\xi = 20, 6.7$, and 4.0 . For comparison, we plot the current density obtained from the gradient expansion, j_θ^{MM} , with $C_0 = \rho$. As the Néel-type skyrmion-vortex always satisfies $\hat{\ell} \perp \text{curl}\hat{\ell}$, this configuration is free from the issue on the anomalous term j^{an} . It is seen from Fig. 4(a) that the current density obtained from the BdG equation is in good agreement with j_θ^{MM} in the weak coupling regime $p_F\xi = 20$, while $j_\theta(r)$ deviates from j_θ^{MM} as $p_F\xi$ decreases. To clarify the Weyl-Bogoliubov quasiparticle contributions, we introduce the E -resolved current density as

$$j_\mu(\mathbf{r}, E) = 2 \sum_{E_i > 0} \left[\text{Im} \left\{ u_{E_i}^*(\mathbf{r}) \partial_\mu u_{E_i}(\mathbf{r}) \right\} \delta(E - E_i) + \text{Im} \left\{ v_{E_i}(\mathbf{r}) \partial_\mu v_{E_i}^*(\mathbf{r}) \right\} \delta(E + E_i) \right], \quad (43)$$

where $E_i \equiv E_n(m, k)$. The current density is obtained by integrating $\mathbf{j}(r, E)$ over E as $j_\mu(\mathbf{r}) = \int dE j_\mu(\mathbf{r}, E) f(E)$. For numerical calculations, the δ -function in Eq. (43) is replaced by the Lorentzian function with the width $0.025\Delta_A$. Figure 4(b) shows the E -resolved current density for the Néel-type skyrmion-vortex at $p_F\xi = 20$. The mass current density may be decomposed into two contributions, $\mathbf{j} = \mathbf{j}^{\text{Weyl}} + \mathbf{j}^{\text{cont}}$. The contribution arising from Weyl-Bogoliubov quasiparticles, \mathbf{j}^{Weyl} , is defined as

$$\mathbf{j}^{\text{Weyl}}(\mathbf{r}) \equiv \int_{-\Delta_A}^{\Delta_A} dE \mathbf{j}(\mathbf{r}, E) f(E), \quad (44)$$

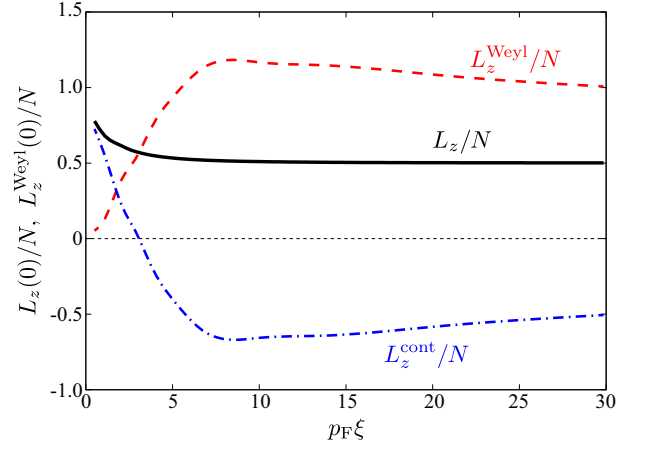


FIG. 5. $p_F\xi$ -dependence of the total angular momentum at $T = 0$: L_z/N (solid line), L_z^{Weyl}/N (dashed line), and L_z^{cont}/N (dashed-dotted line). N is the total particle number, $N = \int n(\mathbf{r})d\mathbf{r}$, and L_z^{Weyl} stands for the contributions of low-lying Weyl-Bogoliubov quasiparticles within $|E_n(m, k)| < \Delta_A$ to the total angular momentum.

and $\mathbf{j}^{\text{cont}} \equiv \mathbf{j} - \mathbf{j}^{\text{Weyl}}$ is the current carried by continuum states. It is seen from Fig. 4(b) that Weyl-Bogoliubov quasiparticle states, including the chiral branch, dominantly contribute to the mass current. However, the continuum states within $|E| > \Delta_A$ make non-vanishing contributions to the mass current. They satisfy $\mathbf{j}^{\text{cont}}(\mathbf{r}) \approx -\mathbf{j}^{\text{Weyl}}/2$ for $p_F\xi \gg 1$, and lead to the counter flow to the Weyl-Bogoliubov quasiparticle flow.

The backflow of the continuum states is also pointed out in the edge mass current with spatially polarized $\hat{\ell}$ -vectors^{64,65} and the surface spin current in the B-phase of the superfluid ^3He .⁶⁶⁻⁶⁸ The main contributions to the mass/spin currents originate in chiral/helical fermion states that are the topologically protected Andreev bound states at the edge. As pointed out by Stone and Roy,⁶⁹ however, the bound states are not the only contribution. Another contribution results from the continuum states affected by the formation of the Andreev bound states. The contribution cancels the bound states, and the edge current arising from the bound states alone differs from the actual edge current by a factor of 2. The E -resolved current density in Fig. 4(b) resembles to the behavior of the edge mass/spin current, where the continuum states are affected by the existence of the nontrivial $\hat{\ell}$ -texture and weakens the flow arising from the chiral fermion states.

To capture the contribution of the Weyl-Bogoliubov quasiparticles more systematically, we calculate the total angular momentum per particle at $T = 0$. The total angular momentum is defined as

$$L_z = \int (\mathbf{r} \times \mathbf{j})_z d\mathbf{r}, \quad (45)$$

and the total particle number is given by $N = \int n(\mathbf{r})d\mathbf{r}$. The angular momentum arising from the Weyl-Bogoliubov quasiparticles within $|E| < \Delta_A$ is given by $L_z^{\text{Weyl}} = \int (\mathbf{r} \times \mathbf{j}^{\text{Weyl}})_z d\mathbf{r}$ and the contribution of the continuum states is $L_z^{\text{cont}} \equiv L_z - L_z^{\text{Weyl}}$. In Fig. 5, we plot the $p_F\xi$ -dependence of the total angular momentum. The total angular momentum in an isolated

Mermin-Ho vortex or a Néel-type skyrmion-vortex was also calculated by Nagai^{70,71} using the quasiclassical theory, which reproduces the McClure-Takagi prediction,⁴⁹ $L_z = \hbar N/2$, at $T \rightarrow 0$. In Fig. 5, the total angular momentum approaches $L_z = \hbar N/2$ at $T = 0$ for $p_F \xi \gg 1$. The angular momentum associated with the Weyl-Bogoliubov quasiparticles differs from the total angular momentum by a factor of 2, which implies the existence of backflow arising from the continuum states, $L_z^{\text{cont}} = -L_z^{\text{Weyl}}/2 = -N\hbar/2$.

In Fig. 5, however, the numerical calculation of the BdG equation in the vicinity of the topological phase transition ($p_F \xi = 0$) shows that L_z/N gradually increases from $\hbar/2$ as $p_F \xi$ decreases. Although L_z/N almost stays constant for $p_F \xi \gtrsim 5$, we find two characteristic behaviors in L_z^{Weyl} and L_z^{cont} ; (i) the Weyl-Bogoliubov quasiparticle contribution, L_z^{Weyl}/N , exhibits the nonmonotonic behavior as a function of $p_F \xi$ and has a maximum around $p_F \xi = 10$. (ii) The continuum contribution, L_z^{cont}/N , changes its sign around $p_F \xi = 3$ and makes a dominant contribution to L_z in $p_F \xi \lesssim 1$. As for (i), the characteristic $p_F \xi$ -dependence of L_z^{Weyl} enables one to discriminate the contribution of TCME from other low-lying quasiparticle contributions. For $p_F \xi \gtrsim 10$, the lower energy part of the angular momentum, L_z^{Weyl} , is approximately decomposed into $L_z^{\text{Weyl}} \sim \hbar N + L_z^{\text{TCME}}$, where $L_z^{\text{TCME}} \equiv \int (\mathbf{r} \times \mathbf{j}^{\text{TCME}})_z d\mathbf{r} \propto 1/(p_F \xi)$ is the angular momentum arising from the torsion-induced current \mathbf{j}^{TCME} in Eq. (23). The TCME vanishes at the weak coupling limit $p_F \xi \gg 1$, while it makes a significant contribution to L_z^{Weyl} as $p_F \xi$ decreases. The contribution of \mathbf{j}^{TCME} is consistent with the increase behavior of L_z^{Weyl} with decreasing $p_F \xi$ within $p_F \xi \gtrsim 10$. We note that the anomalous enhancement of L_z^{Weyl} is compensated by L_z^{cont} and the resultant L_z/N stays constant at $L_z/N = \hbar/2$ for $p_F \xi \gtrsim 10$.

As Eq. (23) is derived from the semiclassical equations of motion for Weyl-Bogoliubov quasiparticles, however, we must be careful about the applicability of Eq. (23). Equation (23) is applicable only to the large $p_F \xi$ regime and fails down in the quantum regime $p_F \xi \sim O(1)$. Figure 5 indeed shows that L_z^{Weyl} vanishes at $p_F \xi = 0$ where the bulk excitation gap closes and topological phase transition occurs.

As we pointed out in (ii), the properties of the mass current and angular momentum in the regime of $p_F \xi \lesssim 10$ are essentially different from those in the quasiclassical limit. The mass current arising from Weyl-Bogoliubov quasiparticles alone weakens with decreasing $p_F \xi$, while high energy quasiparticle states with $|E| > \Delta_A$ make a dominant contribution to L_z/N . In Fig. 6, we plot the T -dependence of L_z/N for $p_F \xi = 10$ and 2.0, where $\Delta_A(T)$ is obtained by calculating the gap equation for a spatially uniform ABM state in Eq. (3). For comparison, we calculate $L_z^{\text{Cross}} = \int (\mathbf{r} \times \mathbf{j}^{\text{Cross}})_z d\mathbf{r}$, which is obtained from the gradient expansion as⁷²

$$\mathbf{j}^{\text{Cross}} = \rho_s \mathbf{v}_s + \frac{\hbar}{4m} \rho_{s\parallel} \text{curl} \hat{\ell} - \frac{\hbar}{2m} \rho_{s\parallel} \hat{\ell} (\hat{\ell} \cdot \text{curl} \hat{\ell}), \quad (46)$$

where $\rho_{s\parallel}$ and $\rho_{s\perp}$ are the components of the superfluid mass density tensor (ρ_s) parallel and perpendicular to $\hat{\ell}$, respectively, and their T -dependencies are determined by the generalized Yosida function.⁷² For the case of $\nabla \rho = \mathbf{0}$, Eq. (46)

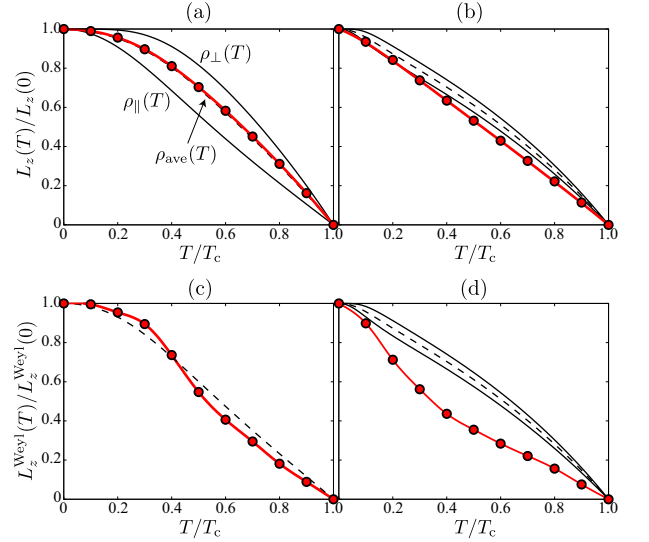


FIG. 6. (a,b) T -dependence of total angular momentum, $L_z(T)$, for the Néel-type skyrmion vortex (red line): (a) $p_F \xi = 20$ and (b) 2.0. (c,d) T -dependence of Weyl-Bogoliubov quasiparticle contributions, $L_z^{\text{Weyl}}(T)$ (red line), for $p_F \xi = 10$ (a) and 2.0 (b). In all figures, the solid lines are the components of the superfluid density tensor parallel and perpendicular to $\hat{\ell}$, ρ_{\parallel} and ρ_{\perp} . The dashed line corresponds to ρ_{ave} , where $\rho_{\text{ave}} = L_z^{\text{Cross}}(T)/L_z^{\text{Cross}}(0)$ for $p_F \xi \gg 1$.

coincides with Eq. (4) at $T = 0$, $\mathbf{j}^{\text{Cross}}(T = 0) = \mathbf{j}^{\text{MM}}$. The averaged superfluid density, $\rho_{\text{ave}} \equiv (\rho_{\perp} + \rho_{\parallel})/2$, describes the T -dependence of $L_z^{\text{Cross}}(T)$ for $p_F \xi \gg 1$, i.e., $L_z^{\text{Cross}}(T)/L_z^{\text{Cross}}(0) = \rho_{\text{ave}}(T)$.

As shown in Fig. 6(a), the T -dependence of $L_z(T)/L_z(0)$ is in good agreement with that of $L_z^{\text{Cross}}(T)/L_z^{\text{Cross}}(0) = \rho_{\text{ave}}(T)$ in the weak coupling regime, $p_F \xi = 10$. As the topological phase transition ($p_F \xi = 0$) is approached, however, the T -dependence of $L_z(T)/L_z(0)$ is distinct from that of $\rho_{\text{ave}}(T)$. In Figs. 6(c) and 6(d), we plot $L_z^{\text{Weyl}}(T)/L_z^{\text{Weyl}}(0)$, the contribution of the Weyl-Bogoliubov quasiparticles to the angular momentum. In $p_F \xi = 10$, the T -dependence is slightly deviated from that of ρ_{ave} and enhanced at the low T regime. This is understandable with an extra contribution of the torsional chiral magnetic effect, L_z^{TCME} , as discussed in Fig. 5. Such extra contribution vanishes as the topological phase transition ($p_F \xi = 0$) is approached and the mass current is dominated by the contribution arising from continuum states.

B. Bloch-type skyrmion

In twisted textures with $\hat{\ell} \cdot \text{curl} \hat{\ell} \neq 0$, the existence of the anomalous term, which is the third term in Eq. (4), has been a long-standing issue. The derivation of Eq. (4) is based on the configuration-space form of the BCS variational ground state wavefunction.⁴⁸ The similar approach was also used by Ishikawa, Miyake, and Usui but came to the different conclusion that the anomalous term, $\mathbf{j}^{\text{an}} \propto \hat{\ell} (\hat{\ell} \cdot \text{curl} \hat{\ell})$, is absent and the resulting mass current is given by $\mathbf{j}^{\text{IMU}} = \mathbf{j}^{\text{MM}} - \mathbf{j}^{\text{an}}$.⁵⁰ As \mathbf{j}^{an} violates the McClure-Takagi relation, the discrepancy

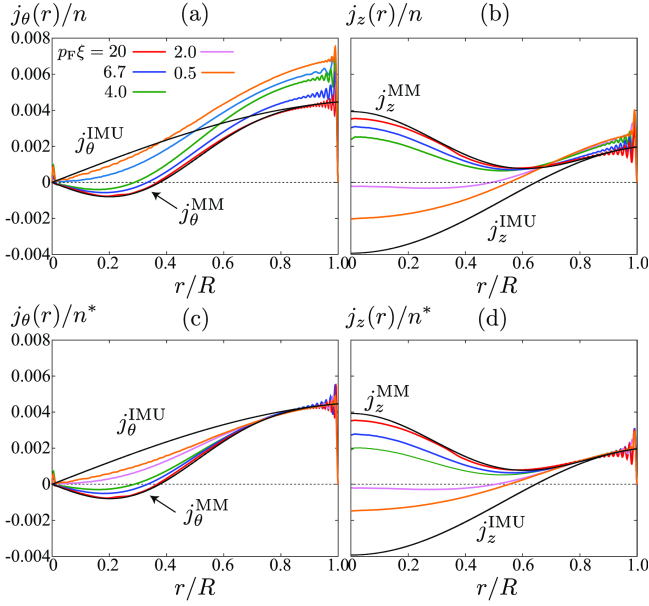


FIG. 7. Current densities in the twisted skyrmion-vortex state at $T = 0$ and $R = 200k_F^{-1}$: (a) azimuthal current $j_\theta(r)/n$ and (b) axial current $j_z(r)/n$. The particle number density n is obtained from the eigenstates of the BdG equation. (c,d) Rescaled current densities, where n^* is a fitting parameter to rescale $j_\mu(r)$ to $j_\mu^{\text{MM}}(R) = j_\mu^{\text{IMU}}(R)$.

between \mathbf{j}^{MM} and \mathbf{j}^{IMU} is referred to as the McClure-Takagi paradox.^{48,51,52} The physical origin of \mathbf{j}^{an} was addressed by Combescot and Dombre^{53,54} and Balatsky *et al.*,^{19,33,34} where the latter unveiled the chiral-anomaly aspect of \mathbf{j}^{an} . Solving the BdG equation in Bloch-type skyrmions, we show below that the mass current is well describable with \mathbf{j}^{MM} in the weak coupling limit, while it approaches \mathbf{j}^{IMU} as the topological phase transition is approached.

Here we consider the mass current induced by Bloch-type twisted-skyrmion textures with $\alpha(r) = \frac{\pi}{2}(1 - r/R)$. Using the particle-hole symmetry, one obtains the current along the axial direction, $j_z(r)$, from Eq. (41) as

$$j_z(r) = 2 \sum_{E < 0} k |u_{mmk}(r)|^2, \quad (47)$$

at $T = 0$. As shown in Fig. 3(b), the Bloch-type skyrmion with the broken P_2 symmetry induces the chiral fermion branches along axial momentum. As the branch has the negative group velocity with respect to k and the $k > 0$ region is occupied at $T = 0$, the asymmetry branch makes a positive contribution to $j_z(r)$. In Fig. 7, we plot the azimuthal and axial currents, $j_\theta(r)$ and $j_z(r)$. In the weak coupling regime ($p_F \xi = 20$), both the current profiles are in good agreement with \mathbf{j}^{MM} including the anomalous term, rather than \mathbf{j}^{IMU} . The total angular momentum per particle is estimated as $L_z(0)/\hbar N = \{0.4490, 0.4361, 0.4339\}$ for $p_F \xi = \{10, 20, 40\}$, respectively. As $p_F \xi$ increases, the values approach $L_z/\hbar N = 0.4336$ obtained from \mathbf{j}^{MM} , but deviate from the McClure-Takagi prediction that $L_z(0)/\hbar N = 0.5$ is independent of the ℓ -texture.⁴⁹ The depletion of $L_z(0)$ from $\hbar N/2$ in the weak coupling regime is consistent with the predictions in Refs. 19, 33, and 34 that

in the Bloch-type twisted skyrmion, the anomalous current arising from the chiral anomaly of Weyl-Bogoliubov quasiparticles makes extra contribution to \mathbf{j} when $\mu > 0$. We note that in contrast to \mathbf{j}^{an} , the torsional contribution, \mathbf{j}^{TCME} , does not give rise to significant deviation of L_z/N in $p_F \xi \rightarrow \infty$, as $\mathbf{j}^{\text{TCME}} \propto 1/(p_F \xi)$.

It is shown in Fig. 7 that the current density deviates from \mathbf{j}^{MM} as the topological phase transition ($p_F \xi = 0$) is approached. To capture the change of the spatial profile in j_θ and j_z , we plot in Figs. 7(c) and 7(d) the rescaled mass current densities, where n^* is a fitting parameter to rescale $j_\mu(r)$ to $j_\mu^{\text{MM}}(R) = j_\mu^{\text{IMU}}(R)$. These figures show that the rescaled profiles gradually shift from \mathbf{j}^{MM} to \mathbf{j}^{IMU} as $p_F \xi$ decreases. This implies that while the contributions of Weyl-Bogoliubov quasiparticles through \mathbf{j}^{an} become significant in the weak coupling regime, \mathbf{j}^{an} and \mathbf{j}^{TCME} become negligible around $p_F \xi \sim 0$.

V. SUMMARY

We have investigated chiral anomaly phenomena induced by skyrmion-like ℓ -textures in the superfluid $^3\text{He-A}$ which is a prototype of Weyl superfluids. Using the semiclassical theory, we have shown the torsional chiral magnetic effect that a torsion field induced by skyrmion-like ℓ -textures results in an equilibrium mass current. In general, the texture of the ℓ -field generates two different emergent fields directly acting on the chirality of Weyl-Bogoliubov quasiparticles: a chiral gauge field ($\mathbf{A} \propto \text{curl} \hat{\ell}$) and a torsion field ($T_{\mu\nu}^a$). In the case of a twisted (Bloch-type skyrmion) ℓ -texture with $\hat{\ell} \cdot \text{curl} \hat{\ell} \neq 0$, the chiral gauge field leads to the extra mass current along $\hat{\ell}$, which is the third term of Eq. (4) referred to as the anomalous current.^{19,30-34,53,54} Here we find the torsional contribution to the mass current. In contrast to the anomalous current, the torsion-induced mass current flows along $\text{curl} \hat{\ell}$ and exists even in the case of Néel-type skyrmion with $\hat{\ell} \cdot \text{curl} \hat{\ell} = 0$.

Using the full quantum mechanical BdG equation, we have demonstrated that in skyrmion vortices a chiral fermion branch with spectral asymmetry appears in the low-lying quasiparticle spectrum. The chiral fermion states are responsible for the equilibrium mass flow. Our numerical results, however, show that the total mass current and the total angular momentum differ from those arising from the chiral fermions alone by a factor of 1/2. The discrepancy is compensated by the backflow arising from the continuum states, and for Néel-type skyrmion vortices, our numerical results in the quasiclassical limit coincide with the prediction by McClure and Takagi,⁴⁹ $L_z = \hbar N/2$. Furthermore, it has been demonstrated that the angular momentum associated with the Weyl-Bogoliubov quasiparticles increase as the topological phase transition ($p_F \xi = 0$) is approached. This anomalous behavior is understandable with the torsional contribution of the current due to the torsional chiral magnetic effect in Eq. (23). We have clarified the torsional-anomaly aspect of the mass current density in Eq. (4); the $\text{curl} \hat{\ell}$ term in Eq. (4) is associated with the TCME of Weyl-Bogoliubov quasiparticles induced by a skyrmion-vortex.

The appearance of a chiral branch in ${}^3\text{He-A}$ was pointed out by Combescot and Dombre,^{53,54} who demonstrated that in the case of a twisted (non-skyrmionic) ℓ -texture ($\hat{\ell} \parallel \text{curl}\hat{\ell}$) the BdG equation for low-lying quasiparticles reduces to the Dirac-type equation with a fictitious magnetic field generated by a variation of the ℓ -field. Balatsky *et al.* clarified that the chiral branch is topologically protected by the Atiyah-Singer index theorem and the chiral fermion carries uncompensated current at $T = 0$.³⁴ Although our result for the mass current qualitatively agrees with that in Ref. 34, it differs from Ref. 34 because they consider only the chiral fermion contributions. As mentioned above, we find that in the quasiclassical limit, the continuum states bring about backflow to the quasiparticle flow, i.e., $L_z^{\text{Weyl}} \approx -2L_z^{\text{cont}} \approx N\hbar$. As the topological phase transition is approached, the mass current carried by the continuum states changes its sign and makes a dominant contribution. In the vicinity of the topological phase transition ($p_{\text{F}}\xi = 0$), indeed, the total angular momentum is governed by

the continuum states and the contribution from chiral fermions is negligible. We have also shown that the contribution of j^{an} is crucial for the weak coupling regime, while it vanishes as $p_{\text{F}}\xi$ decreases. Although L_z/N is composed of the composite contributions of Weyl quasiparticles and continuum states and it is difficult to extract the TCME contribution solely, our results may put a different aspect on the paradox of the mass current and the intrinsic angular momentum.

ACKNOWLEDGMENTS

This work was supported by the Grant-in-Aids for Scientific Research from MEXT of Japan [Grants No. 23540406, No. 25220711, No. JP17K05517, No. JP16K05448, No. JP15H05852, and No. JP15H05855 (KAKENHI on Innovative Areas "Topological Materials Science"), and No. JP18H04318].

-
- ¹ H. Nielsen and M. Ninomiya, *The Adler-Bell-Jackiw anomaly and Weyl fermions in a crystal*, *Phys. Lett. B* **130**, 389 (1983).
 - ² X. Wan, A. M. Turner, A. Vishwanath, and S. Y. Savrasov, *Topological semimetal and Fermi-arc surface states in the electronic structure of pyrochlore iridates*, *Phys. Rev. B* **83**, 205101 (2011).
 - ³ A. A. Burkov and L. Balents, *Weyl Semimetal in a Topological Insulator Multilayer*, *Phys. Rev. Lett.* **107**, 127205 (2011).
 - ⁴ G. B. Halász and L. Balents, *Time-reversal invariant realization of the Weyl semimetal phase*, *Phys. Rev. B* **85**, 035103 (2012).
 - ⁵ S. Murakami, *Phase transition between the quantum spin Hall and insulator phases in 3D: emergence of a topological gapless phase*, *New Journal of Physics* **9**, 356 (2007).
 - ⁶ A. A. Zyuzin and A. A. Burkov, *Topological response in Weyl semimetals and the chiral anomaly*, *Phys. Rev. B* **86**, 115133 (2012).
 - ⁷ P. Goswami and S. Tewari, *Axionic field theory of (3 + 1)-dimensional Weyl semimetals*, *Phys. Rev. B* **88**, 245107 (2013).
 - ⁸ D. T. Son and B. Z. Spivak, *Chiral anomaly and classical negative magnetoresistance of Weyl metals*, *Phys. Rev. B* **88**, 104412 (2013).
 - ⁹ C.-X. Liu, P. Ye, and X.-L. Qi, *Chiral gauge field and axial anomaly in a Weyl semimetal*, *Phys. Rev. B* **87**, 235306 (2013).
 - ¹⁰ M. M. Vazifeh and M. Franz, *Electromagnetic Response of Weyl Semimetals*, *Phys. Rev. Lett.* **111**, 027201 (2013).
 - ¹¹ P. Hosur and X.-L. Qi, *Recent developments in transport phenomena in Weyl semimetals*, *C. R. Phys.* **14**, 857 (2013), [arXiv:1309.4464].
 - ¹² O. Vafek and A. Vishwanath, *Dirac Fermions in Solids: From High-Tc Cuprates and Graphene to Topological Insulators and Weyl Semimetals*, *Annu. Rev. Condens. Matter Phys.* **5**, 83 (2014).
 - ¹³ P. Goswami, J. H. Pixley, and S. Das Sarma, *Axial anomaly and longitudinal magnetoresistance of a generic three-dimensional metal*, *Phys. Rev. B* **92**, 075205 (2015).
 - ¹⁴ N. Yamamoto, *Generalized Bloch theorem and chiral transport phenomena*, *Phys. Rev. D* **92**, 085011 (2015).
 - ¹⁵ S. Jia, S.-Y. Xu, and M. Z. Hasan, *Weyl semimetals, Fermi arcs and chiral anomalies*, *Nat. Mater.* **15**, 1140 (2016).
 - ¹⁶ X. Huang, L. Zhao, Y. Long, P. Wang, D. Chen, Z. Yang, H. Liang, M. Xue, H. Weng, Z. Fang, X. Dai, and G. Chen, *Observation of the Chiral-Anomaly-Induced Negative Magnetoresistance in 3D Weyl Semimetal TaAs*, *Phys. Rev. X* **5**, 031023 (2015).
 - ¹⁷ C.-L. Zhang, S.-Y. Xu, I. Belopolski, Z. Yuan, Z. Lin, B. Tong, G. Bian, N. Alidoust, C.-C. Lee, S.-M. Huang, T.-R. Chang, G. Chang, C.-H. Hsu, H.-T. Jeng, M. Neupane, D. S. Sanchez, H. Zheng, J. Wang, H. Lin, C. Zhang, H.-Z. Lu, S.-Q. Shen, T. Neupert, M. Z. Hasan, and S. Jia, *Signatures of the Adler-Bell-Jackiw chiral anomaly in a Weyl fermion semimetal*, *Nat. Commun.* **7**, 10735 (2016).
 - ¹⁸ T. Meng and L. Balents, *Weyl superconductors*, *Phys. Rev. B* **86**, 054504 (2012).
 - ¹⁹ A. V. Balatsky, G. E. Volovik, and V. A. Konysev, *On the chiral anomaly in superfluid ${}^3\text{He-A}$* , *Zh. Eksp. Teor. Fiz.* **90**, 2038 (1986), [*Sov. Phys. JETP* **63**, 1194 (1986)].
 - ²⁰ G. E. Volovik, *The Universe in a Helium Droplet* (Clarendon, Oxford, 2003).
 - ²¹ G. E. Volovik, *Topology of chiral superfluid: skyrmions, Weyl fermions and chiral anomaly*, *JETP Lett.* **103**, 140 (2016).
 - ²² T. Mizushima, Y. Tsutsumi, T. Kawakami, M. Sato, M. Ichioka, and K. Machida, *Symmetry-Protected Topological Superfluids and Superconductors—From the Basics to ${}^3\text{He}$* , *J. Phys. Soc. Jpn.* **85**, 022001 (2016).
 - ²³ P. Goswami and L. Balicas, *Topological properties of possible Weyl superconducting states of URu_2Si_2* , arXiv:1312.3632 (2013).
 - ²⁴ P. Goswami and A. H. Nevidomskyy, *Topological Weyl superconductor to diffusive thermal Hall metal crossover in the B phase of UPt_3* , *Phys. Rev. B* **92**, 214504 (2015).
 - ²⁵ M. Sato and S. Fujimoto, *Majorana Fermions and Topology in Superconductors*, *J. Phys. Soc. Jpn.* **85**, 072001 (2016).
 - ²⁶ Y. Shimizu, S. Kittaka, S. Nakamura, T. Sakakibara, D. Aoki, Y. Homma, A. Nakamura, and K. Machida, *Quasiparticle excitations and evidence for superconducting double transitions in monocrystalline $\text{U}_{0.97}\text{Th}_{0.03}\text{Be}_{13}$* , *Phys. Rev. B* **96**, 100505 (2017).
 - ²⁷ T. Mizushima and M. Nitta, *Topology and symmetry of surface Majorana arcs in cyclic superconductors*, *Phys. Rev. B* **97**, 024506 (2018).
 - ²⁸ K. Machida, *Spin Triplet Nematic Pairing Symmetry and Superconducting Double Transition in $\text{U}_{1-x}\text{Th}_x\text{Be}_{13}$* ,

- J. Phys. Soc. Jpn. **87**, 033703 (2018).
- ²⁹ T. D. C. Bevan, A. J. Manninen, J. B. Cook, J. R. Hook, H. E. Hall, T. Vachaspati, and G. E. Volovik, *Momentum creation by vortices in superfluid ^3He as a model of primordial baryogenesis*, *Nature* **386**, 689 (1997).
- ³⁰ G. E. Volovik and V. P. Mineev, *Orbital angular momentum and orbital dynamics: $^3\text{He-A}$ and the Bose liquid*, *Zh. Eksp. Teor. Fiz.* **81**, 989 (1981), [*Sov. Phys. JETP* **56**, 579 (1982)].
- ³¹ G. E. Volovik, *Superfluid properties of $^3\text{He-A}$* , *Usp. Fiz. Nauk* **143**, 73 (1984), [*Sov. Phys. Usp.* **27**, 363 (1984)].
- ³² G. E. Volovik, *Normal Fermi liquid in a superfluid $^3\text{He-A}$ at $T = 0$ and the anomalous current*, *Pi'sma Zh. Eksp. Teor. Fiz.* **42**, 294 (1985), [*JETP Lett.* **42**, 363 (1985)].
- ³³ G. E. Volovik, *Chiral anomaly and the law of conservation of momentum in $^3\text{He-A}$* , *Pi'sma Zh. Eksp. Teor. Fiz.* **43**, 428 (1986), [*JETP Lett.* **43**, 551 (1986)].
- ³⁴ A. V. Balatsky and V. A. Konysev, *The anomalous superfluid current in $^3\text{He-A}$ and the index theorem*, *Zh. Eksp. Teor. Fiz.* **92**, 841 (1987), [*Sov. Phys. JETP* **65**, 474 (1987)].
- ³⁵ G. E. Volovik, *Orbital angular momentum of vortices and textures due to spectral flow through the gap nodes: example of the $^3\text{He-A}$ continuous vortex*, *Pi'sma Zh. Eksp. Teor. Fiz.* **61**, 935 (1995), [*JETP Lett.* **61**, 958 (1995)].
- ³⁶ H. Sumiyoshi and S. Fujimoto, *Torsional Chiral Magnetic Effect in a Weyl Semimetal with a Topological Defect*, *Phys. Rev. Lett.* **116**, 166601 (2016).
- ³⁷ T. Kobayashi, T. Matsushita, T. Mizushima, A. Tsuruta, and S. Fujimoto, *Negative Thermal Magnetoresitivity as a Signature of Chiral Anomaly in Weyl Superconductors*, arXiv:1806.00993 (2018).
- ³⁸ P. W. Anderson and P. Morel, *Generalized Bardeen-Cooper-Schrieffer States and the Proposed Low-Temperature Phase of Liquid He^3* , *Phys. Rev.* **123**, 1911 (1961).
- ³⁹ P. W. Anderson and W. F. Brinkman, *Anisotropic Superfluidity in ^3He : A Possible Interpretation of Its Stability as a Spin-Fluctuation Effect*, *Phys. Rev. Lett.* **30**, 1108 (1973).
- ⁴⁰ M. M. Salomaa and G. E. Volovik, *Quantized vortices in superfluid ^3He* , *Rev. Mod. Phys.* **59**, 533 (1987).
- ⁴¹ O. V. Lounasmaa and E. Thuneberg, *Vortices in rotating superfluid ^3He* , *Proc. Natl. Acad. Sci.* **96**, 7760 (1999).
- ⁴² V. Eltsov, M. Krusius, and G. Volovik, *Vortex formation and dynamics in superfluid ^3He and analogies in quantum field theory*, in *Progress in Low Temperature Physics*, Vol. 15, edited by W. Halperin (Elsevier, 2005) pp. 1 – 137.
- ⁴³ D. Vollhardt and P. Wölfle, *The Superfluid Phases of Helium 3* (Taylor and Francis, London, 1990).
- ⁴⁴ N. D. Mermin and T.-L. Ho, *Circulation and Angular Momentum in the A Phase of Superfluid Helium-3*, *Phys. Rev. Lett.* **36**, 594 (1976).
- ⁴⁵ P. W. Anderson and G. Toulouse, *Phase Slippage without Vortex Cores: Vortex Textures in Superfluid ^3He* , *Phys. Rev. Lett.* **38**, 508 (1977).
- ⁴⁶ J. J. Wiman and J. A. Sauls, *Superfluid phases of ^3He in nanoscale channels*, *Phys. Rev. B* **92**, 144515 (2015).
- ⁴⁷ J. J. Wiman and J. A. Sauls, *Spontaneous Helical Order of a Chiral p-Wave Superfluid Confined in Nanoscale Channels*, *Phys. Rev. Lett.* **121**, 045301 (2018).
- ⁴⁸ N. D. Mermin and P. Muzikar, *Cooper pairs versus Bose condensed molecules: The ground-state current in superfluid $^3\text{He-A}$* , *Phys. Rev. B* **21**, 980 (1980).
- ⁴⁹ M. G. McClure and S. Takagi, *Angular Momentum of Anisotropic Superfluids*, *Phys. Rev. Lett.* **43**, 596 (1979).
- ⁵⁰ M. Ishikawa, K. Miyake, and T. Usui, *Intrinsic Angular Momentum and Mass Current in Superfluid $^3\text{He-A}$* , *Prog. Theor. Phys.* **63**, 1083 (1980).
- ⁵¹ T. Kita, *The Angular Momentum Paradox of $^3\text{He-A}$* , *J. Phys. Soc. Jpn.* **65**, 664 (1996).
- ⁵² A. Tsuruta, S. Yukawa, and K. Miyake, *Intrinsic Angular Momentum and Intrinsic Magnetic Moment of Chiral Superconductor on Two-Dimensional Square Lattice*, *J. Phys. Soc. Jpn.* **84**, 094712 (2015).
- ⁵³ R. Combescot and T. Dombre, *Superfluid current in $^3\text{He-A}$ at $T = 0$* , *Phys. Rev. B* **28**, 5140 (1983).
- ⁵⁴ R. Combescot and T. Dombre, *Twisting in superfluid ^3A and consequences for hydrodynamics at $T=0$* , *Phys. Rev. B* **33**, 79 (1986).
- ⁵⁵ R. Takashima and S. Fujimoto, *Supercurrent-induced skyrmion dynamics and tunable Weyl points in chiral magnet with superconductivity*, *Phys. Rev. B* **94**, 235117 (2016).
- ⁵⁶ M. A. Stephanov and Y. Yin, *Chiral Kinetic Theory*, *Phys. Rev. Lett.* **109**, 162001 (2012).
- ⁵⁷ H. Kleinert, *Classical and Fluctuating Paths in Spaces with Curvature and Torsion*, arXiv:quant-ph/9606001 (1996).
- ⁵⁸ T. Mizushima and K. Machida, *Vortex structures and zero-energy states in the BCS-to-BEC evolution of p-wave resonant Fermi gases*, *Phys. Rev. A* **81**, 053605 (2010).
- ⁵⁹ M. Matsumoto and R. Heeb, *Vortex charging effect in a chiral $p_x \pm ip_y$ -wave superconductor*, *Phys. Rev. B* **65**, 014504 (2001).
- ⁶⁰ F. Gygi and M. Schlüter, *Self-consistent electronic structure of a vortex line in a type-II superconductor*, *Phys. Rev. B* **43**, 7609 (1991).
- ⁶¹ M. M. Salomaa and G. E. Volovik, *Symmetry and structure of quantized vortices in superfluid ^3B* , *Phys. Rev. B* **31**, 203 (1985).
- ⁶² M. M. Salomaa and G. E. Volovik, *Vortices with Ferromagnetic Superfluid Core in $^3\text{He-B}$* , *Phys. Rev. Lett.* **51**, 2040 (1983).
- ⁶³ M. Ichioka, T. Mizushima, and K. Machida, *Skyrmion lattice and intrinsic angular momentum effect in the A phase of superfluid ^3He under rotation*, *Phys. Rev. B* **82**, 094516 (2010).
- ⁶⁴ J. A. Sauls, *Surface states, edge currents, and the angular momentum of chiral p-wave superfluids*, *Phys. Rev. B* **84**, 214509 (2011).
- ⁶⁵ Y. Tsutsumi and K. Machida, *Edge mass current and the role of Majorana fermions in A-phase superfluid ^3He* , *Phys. Rev. B* **85**, 100506 (2012).
- ⁶⁶ H. Wu and J. A. Sauls, *Majorana excitations, spin and mass currents on the surface of topological superfluid $^3\text{He-B}$* , *Phys. Rev. B* **88**, 184506 (2013).
- ⁶⁷ Y. Tsutsumi and K. Machida, *Edge Current due to Majorana Fermions in Superfluid ^3He A- and B-Phases*, *J. Phys. Soc. Jpn.* **81**, 074607 (2012).
- ⁶⁸ T. Mizushima, Y. Tsutsumi, M. Sato, and K. Machida, *Symmetry protected topological superfluid $^3\text{He-B}$* , *J. Phys.: Condens. Matter* **27**, 113203 (2015).
- ⁶⁹ M. Stone and R. Roy, *Edge modes, edge currents, and gauge invariance in p_x+ip_y superfluids and superconductors*, *Phys. Rev. B* **69**, 184511 (2004).
- ⁷⁰ K. Nagai, Y. Nagato, and S. Higashitani, *Low Temperature Properties of the Mermin-Ho Texture of Superfluid $^3\text{He-A}$ in a Cylinder*, *J. Phys.: Conf. Ser.* **400**, 012054 (2012).
- ⁷¹ K. Nagai, *Quasi-classical Theory of the A-phase of Superfluid $^3\text{He-A}$ in a Cylinder*, *J. Low Temp. Phys.* **175**, 44 (2014).
- ⁷² M. Cross, *A generalized Ginzburg-Landau approach to the superfluidity of helium 3*, *J. Low Temp. Phys.* **21**, 525 (1975).